Estimation of delay in coupling from time series

Laura Cimponeriu,[1,*] Michael Rosenblum,[2] and Arkady Pikovsky[2]
[1]*Department of Medical Physics, University of Patras, 26 500 Rion Patras, Greece*
[2]*Department of Physics, University of Potsdam, Postfach 601553, D-14415 Potsdam, Germany*
(Received 20 May 2004; published 25 October 2004)

We demonstrate that a time delay in weak coupling between two self-sustained oscillators can be estimated from the observed time series data. We present two methods which are based on the analysis of interrelations between the phases of the signals. We show analytically and numerically that irregularity of the phase dynamics (due to the intrinsic noise or chaos) is essential for determination of the delay. We compare and contrast both methods to the standard cross-correlation analysis.

DOI: 10.1103/PhysRevE.70.046213 PACS number(s): 05.45.Tp, 05.45.Xt, 02.50.Ey

I. INTRODUCTION

Many natural phenomena can be described by coupled oscillator models. Quite often there exists a certain *time delay in coupling*, which can, e.g., significantly influence the dynamical behavior and synchronization properties [1–6]. Indeed, in many cases the propagation time of a signal through a pathway connecting the interacting subsystems is not small compared to the characteristic oscillation period, and, hence, the delay in coupling must be taken into account. Examples include laser systems [7], a living coupled oscillator system with the plasmodium of *Physarum polycephalum* [8], cardiorespiratory system [9], and neuronal populations [10–12].

In this paper we address the problem whether the delay in *weak coupling* of noisy limit cycle or chaotic oscillators can be estimated from the time series of the processes. Note that the problem is nontrivial, because the dynamical behavior (e.g., a synchronization pattern) in the presence of delay in coupling may be quite similar to that of instantaneously coupled systems. We demonstrate that, counterintuitively, identification of the time delay is possible if the interacting oscillators are sufficiently *noisy*. Noise plays a constructive role because it breaks the coherence between the current and delayed states, and therefore allows us to distinguish them. A similar role can be played by chaos; see [13–21] for a description of methods for estimation of internal delay in a nonlinear system exhibiting chaotic dynamics and [22] for the treatment of a linear stochastic system. We also discuss the distinction between the delay and the phase difference of two signals and emphasize that in the case we analyze here the delay cannot be accurately estimated by means of cross-correlation or cross-spectral analysis.

The input to the algorithms proposed in this paper are the series of instantaneous phases. As is usually done in synchronization analysis of multivariate data [23,24], we assume that we can measure the signals on the outputs of interacting oscillators and that these signals are appropriate for determination of the instantaneous phases; for a description and discussion of phase estimation techniques see [23,24].

The paper is organized as follows. In Sec. II we present the methods for delay estimation and in Sec. III we analyze them analytically. In Sec. IV we consider numerical examples illustrating that the delay in coupling between noisy and/or chaotic oscillators can be estimated from the series of instantaneous phases. In Sec. V we discuss our results.

II. PHASE MODEL AND METHODS FOR DELAY ESTIMATION

As is well known, the description of weakly coupled self-sustained oscillators can be in a good approximation reduced to the phase dynamics [24,25]. Hence, in the following theoretical analysis we consider coupled phase oscillators described by the following general equations:

$$\dot{\phi}_1 = \omega_1 + \varepsilon F_1(\phi_1(t), \phi_2(t - T_{12})) + \xi_1(t), \qquad (1)$$

$$\dot{\phi}_2 = \omega_2 + \varepsilon F_2(\phi_1(t - T_{21}), \phi_2(t)) + \xi_2(t),$$

where $\phi_{1,2}$ and $\omega_{1,2}$ are phases and natural frequencies of two oscillators, respectively, and $\xi_{1,2}$ are noisy terms, whereas T_{12} and T_{21} are time delays in coupling. Model (1) describes coupled noisy limit cycle oscillators as well as some chaotic systems [24] ; in the latter case the irregular terms $\xi_{1,2}$ reflect the chaotic amplitude dynamics. For clarity of presentation and simplicity of the analytical treatment we first concentrate on the case of two unidirectionally coupled systems with the simplest coupling function:

$$\dot{\phi}_1 = \omega_1 + \varepsilon \sin[\phi_2(t - T) - \phi_1(t) - \alpha] + \xi_1(t), \qquad (2)$$

$$\dot{\phi}_2 = \omega_2 + \xi_2(t),$$

where α is a constant phase shift. Here we assume that the noisy forces perturbing two oscillators are Gaussian, independent and δ correlated $\langle \xi_{1,2}(t)\xi_{1,2}(t+\tau)\rangle = 2D_{1,2}\delta(\tau)$, $\langle \xi_1(t)\xi_2(t+\tau)\rangle = 0$. Later, in Sec. IV we explain qualitatively and confirm numerically the validity of our approach for bidirectional coupling and more general coupling functions F_1, F_2 as well.

We discuss first possible types of dynamical behavior in system (2). The most important effect here is synchroniza-

*Present address: Center for Research and Applications of Nonlinear Systems (CRANS), University of Patras, Greece.

tion: for sufficiently large coupling strength ε and for vanishing noise there is a stable solution with a constant phase shift between the oscillators. It is easy to show that for $\varepsilon \geqslant |\omega_1 - \omega_2|$ there exist a synchronous solution with a constant phase difference

$$\psi_0 = \phi_2(t) - \phi_1(t) = \arcsin\left(\frac{\omega_2 - \omega_1}{\varepsilon}\right) + \omega_2 T + \alpha. \quad (3)$$

For $\varepsilon < |\omega_1 - \omega_2|$, Eqs. (2) exhibit quasiperiodicity, when the phase difference grows with time. If noise is present, the perfect synchrony is destroyed: the phase difference exhibits small fluctuations around ψ_0 with possible relatively rapid 2π jumps (phase slips). In a quasiperiodic state, fluctuations are superimposed on the deterministic growth of the phase difference due to the detuning between the oscillators (see, e.g., [24] for details).

It is important that if the noise in the driver ξ_2 is absent, then the delay time T cannot be inferred. Indeed, let us assume that the form of the coupling function in Eqs. (2) is known exactly, but its parameters ε and α are unknown. We see that the delay and phase shift α appear in the argument of the sine function as a combination $\omega_2 T + \alpha$. Hence, in the purely deterministic case there is no way to distinguish between two different delays T' and T'', because α can be arbitrary and therefore the condition $\omega_2 T' + \alpha' = \omega_2 T'' + \alpha''$ can be always fulfilled. Moreover, we emphasize that the delay in coupling cannot be inferred from the observation of the phase shift ψ_0 between synchronized oscillators. Indeed, in the synchronous regime both phases grow in time with a common rate [$\omega_2 t$ in the example of system (2)] and differ by a constant ψ_0 that is determined by the detuning $\omega_2 - \omega_1$, parameters of coupling ε and α, and delay T (the latter two appear again as the combination $\omega_2 T + \alpha$), and the contribution of these factors cannot be separated. Hence, measurements of the phase difference cannot provide the estimate of the delay, as sometimes is assumed in physiological and medical literature;[1] indeed, the presence of the delay generally implies presence of a (constant in average) phase difference, but not vice versa.

Below we demonstrate that noise plays a constructive role in the context of determination of a delayed interaction. So, in system (2), the noise ξ_2 breaks the coherence of the phase ϕ_2 and therefore the time delay is not equivalent to the phase shift. In the rest of this paper we develop and discuss the methods for determination of the delay time in the coupling from the observation of the phases $\phi_1(t)$ and $\phi_2(t)$ under assumption that their evolution can be approximated by Eqs. (1).

A. Delay estimation based on a synchronization index

In this method it is assumed that the oscillators are nearly synchronized; i.e., the phase difference between the oscillators most of the time exhibits small fluctuations around a stable value [cf. Eq. (3)], possibly intermingled with rare phase slips—i.e., relatively rapid jumps when the phase difference gains $\pm 2\pi$. Consequently, there is a high correlation between the values of $\phi_1(t)$ and $\phi_2(t-T)$, as the retarded value of ϕ_2 directly governs the phase ϕ_1. On the other hand, the correlation between $\phi_1(t)$ and $\phi_2(t-\tau)$ for $\tau \neq T$ is expected to be smaller. To quantify this, one can characterize the relation between two *shifted-in-time* time series of phases $\phi_{1,2}$ by a *shift-dependent synchronization index* [26]

$$\rho^2(\tau) = \langle \cos[\phi_1(t) - \phi_2(t-\tau)] \rangle^2 + \langle \sin[\phi_1(t) - \phi_2(t-\tau)] \rangle^2, \quad (4)$$

where $\langle\rangle$ denote averaging over time. For the shift $\tau = 0$ the index reduces to the index used in synchronization analysis for characterization of the strength of phase interrelation between two signals [23,27]. One can expect that $\rho(\tau)$ has a maximum at $\tau = T$. However, this is not exactly true: as we show theoretically in Sec. III A and confirm numerically in Sec. IV below, the position of the maximum of the dependence of the synchronization index ρ on the time shift τ systematically overestimates the delay. Moreover, in the case when the oscillators are far from synchrony, the synchronization index is small for all shifts τ and therefore does not yield the estimate of the delay. Thus, the advantages of this approach—namely, its simplicity and absence of parameters—are accompanied by several drawbacks which can be overcome by the technique presented below in Sec. II C.

B. Cross-correlation function

The most common tool that can be tested for the detection of the delay is the cross-correlation function. Given the time series of phases, the (normalized) cross-correlation function between the two oscillations is calculated for the observables $\cos\phi_1$ and $\cos\phi_2$ as

$$C(\tau) = 2\langle \cos[\phi_1(t)] \cos[\phi_2(t-\tau)] \rangle,$$

where the fluctuations of the amplitudes are neglected. Assuming that the systems are close to synchrony, we can express the phases as $\phi_{1,2} = \omega(t - t_0) + \varphi_{1,2}$, where ω is some frequency of order $\omega \approx (\omega_1 + \omega_2)/2$ [it is $\omega = \omega_2$ for unidirectional coupling described by Eqs. (2)] and $\varphi_{1,2}$ are slow phases. In the computation, we have to average over the ensemble of realizations with random initial times t_0; hence, the terms containing $\sin\omega t_0$ and $\cos\omega t_0$ vanish. With the introduced notations we obtain

$$\begin{aligned} C(\tau) &= 2\langle \cos[\omega(t-t_0) + \varphi_1(t)] \cos[\omega(t-t_0) - \omega\tau \\ &\quad + \varphi_2(t-\tau)] \rangle \\ &= \langle \cos[\varphi_1(t) - \varphi_2(t-\tau) + \omega\tau] \rangle \\ &= \cos\omega\tau \langle \cos[\varphi_1(t) - \varphi_2(t-\tau)] \rangle \\ &\quad - \sin\omega\tau \langle \sin[\varphi_1(t) - \varphi_2(t-\tau)] \rangle \\ &= A(\tau)\cos(\omega\tau + \alpha), \end{aligned}$$

[1] In a number of papers the phase of the cross spectrum at a dominating frequency is recomputed into a delay. Our consideration shows that this procedure, appropriate for input-output systems, fails in case of coupled self-sustained oscillators.

where the envelope of the cross-correlation function is defined via

$$A^2(\tau) = \langle \cos[\varphi_1(t) - \varphi_2(t-\tau)]\rangle^2 + \langle \sin[\varphi_1(t) - \varphi_2(t-\tau)]\rangle^2$$

and $\cos\alpha = \langle \cos[\varphi_1(t) - \varphi_2(t-\tau)]\rangle / A$. Noting that $\phi_1(t) - \phi_2(t-\tau) = \varphi_1(t) - \varphi_2(t-\tau) + \text{const}$ and comparing with Eq. (4) we obtain

$$A(\tau) = \rho(\tau).$$

Note, however, that if the fluctuations of the amplitudes of the observables $x_1(t)$ and $x_2(t)$ are not small, then the envelope of the cross-correlation function of these processes can essentially deviate from the synchronization index (cf. Fig. 2 below).

C. Delay estimation based on model fitting

This approach to delay estimation is based on the reconstruction of the first equation in Eqs. (2) from the series $\phi_{1,2}$. Namely, we suggest to fit the numerically estimated phase derivative $d\phi_1/dt$—that is, the instantaneous frequency of the first oscillator—by a function of $\phi_1(t)$ and $\phi_2(t-\tau)$, for different values of the shift τ.[2] Practically, we try to fit the finite-difference estimation of the derivative $[\phi_1(t+\Delta t) - \phi_1(t)](\Delta t)^{-1}$ with a probe function in the form of the double Fourier series in $\phi_{1,2}$, because in general case the coupling function is 2π periodic in $\phi_{1,2}$. The quality of the fit is characterized by the least-mean-squares error E. The idea of the approach is that the dependence $E(\tau)$ should take a minimum at $\tau = T$. This is confirmed by the theoretical analysis of this method, performed in Sec. III B, whereas the technical details and numerical illustration of the approach can be found in Sec. IV.

III. THEORETICAL ANALYSIS OF THE METHODS

In this section we present an analytical derivation of the above defined quantities $\rho(\tau)$ and $E(\tau)$ for the basic model (2) and discuss under which conditions they allow us to determine the delay in the coupling.

A. Synchronization index

Writing the second equation Eqs. (2) for the delayed time as $\dot\phi_2(t-T) = \omega_2 + \xi_2(t-T)$, we obtain for the phase difference

$$\psi = \phi_1(t) - \phi_2(t-T) \tag{5}$$

the stochastic Adler equation

$$\dot\psi = \nu - \varepsilon\sin(\psi + \alpha) + \xi_1(t) - \xi_2(t-T), \tag{6}$$

where $\nu = \omega_1 - \omega_2$ is the detuning. The probability distribution $P(\psi)$ for the solution of this equation can be found in [24,28], with the amplitude of the first harmonics giving the synchronization index $P_1(\psi) = \rho(T)$.

[2]We note that in a practical situation we do not have to know *a priori* which system is the driver; see Sec. IV.

Consider now the synchronization index $\rho(\tau)$ for $\tau \neq T$. In order to compute it, we have to find the probability distribution of

$$\theta = \phi_1(t) - \phi_2(t-\tau) = \psi + (T-\tau)\omega_2 + \eta, \tag{7}$$

where

$$\eta = \int_{t-\tau}^{t-T} \xi_2(s)\,ds \tag{8}$$

is a Gaussian random number with zero mean and variance $2D_2|T-\tau|$. If ψ and η were independent (this can be taken as a zero approximation), then the distribution of θ would be the convolution of the distributions for ψ and η. In the Fourier domain we can multiply the Fourier transforms, which gives, for the first harmonics of the distribution,

$$P_1(\theta) = P_1(\psi)\exp(-D_2|T-\tau|)$$

or

$$\rho(\tau) = \rho(T)\exp(-D_2|T-\tau|). \tag{9}$$

It can be seen that the synchronization index has a maximum at $\tau = T$; however, in the absence of the noise in the driver ($D_2 = 0$) the synchronization index becomes independent of τ.

To account for correlations we assume that the coupling is sufficiently strong, so that the fluctuations around the synchronous state are small. In this case we can linearize the Adler equation (6) around the constant synchronous value $\psi_0 = \arcsin(\nu/\varepsilon) - \alpha$ and write an equation for the small deviation of the phase difference $\Psi = \psi - \psi_0$:

$$\dot\Psi = -A\Psi + \xi_1(t) - \xi_2(t-T), \tag{10}$$

where

$$A = \varepsilon\,\cos(\psi_0 + \alpha) = \sqrt{\varepsilon^2 - \nu^2}. \tag{11}$$

Statistical analysis of this model, details of which are presented in Appendix A, leads to the following expression:

$$\rho(\tau) = e^{-(D_1+D_2)/A} e^{-D_2|T-\tau|} \times \begin{cases} \exp\left(\dfrac{2D_2}{A}(1 - e^{-(\tau-T)A})\right), & \tau \geqslant T, \\ 1, & \tau < T. \end{cases} \tag{12}$$

This function has only one maximum, which occurs in domain of the argument $\tau_{\max} > T$. Thus, synchronization index attains its maximum value for $\tau = \tau_{\max}$ found from the condition

$$-D_2 + 2D_2 e^{-(\tau_{\max}-T)A} = 0.$$

Provided the phase of the driver diffuses, $D_2 > 0$, this gives, with account of Eq. (11),

$$\tau_{max} = T + \ln 2/A = T + \frac{\ln 2}{\sqrt{\varepsilon^2 - \nu^2}}. \tag{13}$$

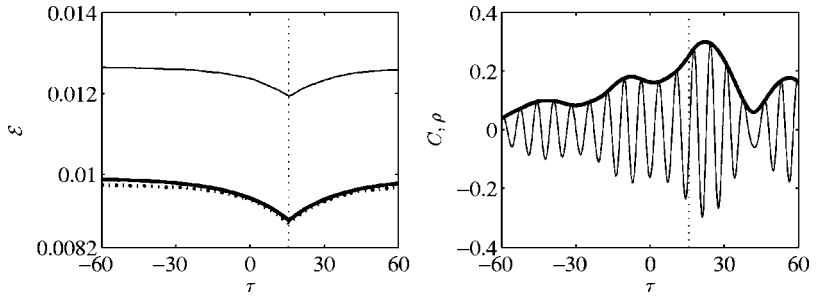

FIG. 1. Estimation of the delay in coupling of noisy limit cycle oscillators [Eqs. (18)]. The dotted vertical lines mark the true value of the delay T. Left panel: error of the fit $\mathcal{E}$ as the function of shift τ, computed from the phases obtained via the Hilbert transform (solid line) and from the phases obtained directly from Eqs. (18) (dotted line), as well as the theoretical curve according to Eq. (17) (bold line). Right panel: dependence of the synchronization index ρ on the shift τ (bold line) and the cross-correlation function (solid line); $\rho(\tau)$ nearly coincides with the envelope of $C(\tau)$. Note that $\rho(\tau)$ dependence provides a biased estimate of the delay.

Thus, the described method produces a biased estimate of the delay, where the bias decreases with the increase of the driving strength; cf. the numerical results shown in Figs. 3 and 4.

B. Error of model fitting

In this method we try to approximate the right-hand side (RHS) of the first equation in Eqs. (2), i.e.,

$$f(\phi_1(t),\phi_2(t-T)) = \omega_1 + \varepsilon \sin[\phi_2(t-T) - \phi_1(t) - \alpha] + \xi_1(t) = \omega_1 - \varepsilon \sin(\psi + \alpha) + \xi_1(t), \quad (14)$$

by a function of $\phi_1(t)$ and $\phi_2(t-\tau)$, where τ can be positive or negative. Let our test function be

$$f'(t) = \omega' + \varepsilon' \sin[\phi_2(t-\tau) - \phi_1(t) - \tilde{\alpha}'].$$

Using Eq. (7) and denoting $\alpha' = \tilde{\alpha}' + (T-\tau)\omega_2$ we rewrite it as

$$f'(t) = \omega' - \varepsilon' \sin(\psi + \eta + \alpha'). \quad (15)$$

Determination of the parameters $\omega', \varepsilon', \alpha'$ by least-mean-squares fitting leads to an expression for the error of the fit. This expression can be obtained analytically for two limit cases: (i) the oscillators are far from synchrony and (ii) the oscillators are very close to synchrony; the calculations for both cases are given in Appendix B. In the first case we end with the following expression for the error of the fit [see Eq. (B1)]:

$$E^2(\tau) = \frac{\varepsilon^2}{2}(1 - e^{-2D_2|T-\tau|}) + \langle \xi_1^2 \rangle. \quad (16)$$

This error as a function of τ has a minimum at $\tau = T$. Thus we obtain an estimate of the delay T as an output of the fitting procedure. The stronger the coupling and the phase diffusion in the driver, the more pronounced is the minimum. Its position provides the unbiased estimate of the delay, contrary to the estimate provided by the position of the maximum of the synchronization index. In the close to synchrony case the error of the fit as a function of shift $E(\tau)$ also has a sharp minimum for $T = \tau$; the lengthy expression for $E(\tau)$ is given by Eq. (B2) in Appendix B and illustrated in Fig. 10.

Note that in Eqs. (16) and (B2) the noise intensity $\langle \xi_1^2 \rangle$ appears as an additive constant. Formally, for δ-correlated noise this quantity diverges. However, this is not important because practically we fit not the derivative of the phase but its finite-difference approximation $[\phi_1(t+\Delta t) - \phi_1(t)](\Delta t)^{-1}$. For the Langevin equation with δ-correlated noise such an estimation contains a regular term that is Δt independent and a noisy term $\sim(\Delta t)^{-1/2}$. Therefore, the Eq. (16) becomes

$$E^2(\tau) = \frac{\varepsilon^2}{2}(1 - e^{-2D_2|T-\tau|}) + \frac{2D_1}{\Delta t}. \quad (17)$$

[The same consideration is valid for Eq. (B2).] Thus, the error of the fit as a function of the shift $E(\tau)$ contains two components: the first, the regular one, is independent of Δt and is determined by the proper choice of the shift τ. On the contrary, the contribution of the noisy term is τ independent and decreases with Δt. Hence, the variation of E within a given range of shift τ; i.e., $E^2_{max} - E^2_{min}$, is approximately constant, while E^2_{min} is inversely proportional to Δt. Correspondingly, the relative variation of the error for the given range of τ will be larger for larger Δt. In order to preserve accuracy of the estimation of the delay time the interval Δt should be, however, kept small compared to the delay.

IV. NUMERICAL RESULTS

We start with a discussion of general aspects of numerical implementation of the described methods. The calculation of the cross-correlation function is standard. For the synchronization index estimation (SIE) and model fitting estimation (MFE) methods one has first to compute the phases from scalar signals; in all examples below this has been done with the help of the analytic signal method based on the Hilbert transform (see [23,24]). The calculation of $\rho(\tau)$ is then straightforward, whereas the computation of $E(\tau)$ requires a discussion.

The first important point is the substitution of the derivative $\dot{\phi}_1$ by the finite difference $[\phi_1(t+\Delta t) - \phi_1(t)](\Delta t)^{-1}$. Namely, we compute the error of the fit $\mathcal{E} = E\Delta t$ for the *phase increment* $\Delta\phi_1(t) = \phi_1(t+\Delta t) - \phi_1(t)$. In this way we avoid the poor operation of numerical derivation of a noisy time series. Moreover, as discussed above, by increasing Δt we effectively filter out the internal noise of a driven oscillator. Note that for practical purposes, when there is no need for

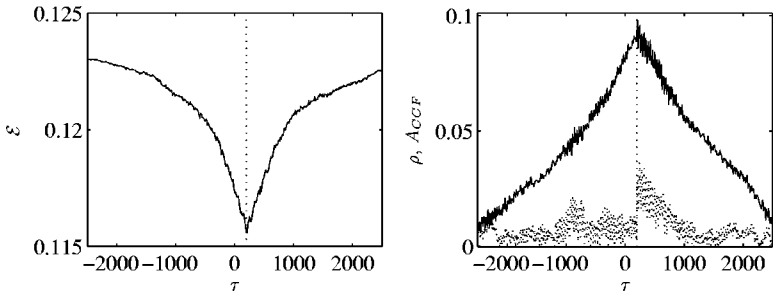

FIG. 2. Unidirectional delayed coupling of chaotic Rössler oscillators [Eqs. (19)]. The delay in coupling is estimated from the position of the minimum of $\mathcal{E}(\tau)$ and maximum of $\rho(\tau)$. The dashed curve in the right panel shows the envelope of the cross-correlation function between x_1 and x_2.

comparison of theoretical results with numerics, it is convenient to use the *normalized error* $\mathcal{E}_N$. The latter is computed for the phase increments normalized by their rms value; $\mathcal{E}_N$ varies from zero to 1.

Another important issue is the choice of the fitting function. The natural choice here is a Fourier series. As soon as the number of terms of this series has been chosen, the error of fit $E(\tau)$ is obtained via a standard linear regression procedure. With a little effort the significant Fourier terms can be determined by trial and error—namely, by checking that no systematic periodic distribution is displayed by the residuals. Alternatively, the dominant terms can be revealed by means of the procedure described in Appendix C.

A. Unidirectional coupling

We start our numerical simulations with a consideration of two coupled noisy limit cycle oscillators described by the Landau-Stuart equations

$$\dot{A}_1(t) = (1 + i\omega_1)A_1(t) - |A_1(t)|^2 A_1(t) - \varepsilon A_2(t - T) + \xi_1(t),$$
$$\dot{A}_2(t) = (1 + i\omega_2)A_2(t) - |A_2(t)|^2 A_2(t) + \xi_2(t), \tag{18}$$

where $A_{1,2}$ represent the complex amplitude variables, $\omega_{1,2} = 1 \pm \Delta\omega$ are the natural frequencies of the oscillators, ε is the strength of coupling, and $\xi_{1,2}(t)$ denote the Gaussian δ-correlated noises of intensities $2D_{1,2}$. Numerical integration of Eqs. (18) has been performed using a fixed-step-size ($h = 2\pi/100$) stochastic Euler scheme. The parameters of the system are $\Delta\omega = 0.1$, $\varepsilon = 0.1$, $T = 250h \approx 15.7$, $\sqrt{2D_1} = 0.05$, and $\sqrt{2D_2} = 0.3$. The results are presented in Fig. 1. They demonstrate that a delay in (weak) coupling can be revealed both by the MFE and SIE algorithms. However, the latter approach provides a *biased estimate*. Here in the left panel we show the $E(\tau)$ curve computed from the Hilbert phases $\phi_H = \arg[\mathrm{Re}(A) + i\mathcal{H}(\mathrm{Re}(A))]$, where $\mathcal{H}(\cdot)$ denotes the Hilbert transform, as well as the $E(\tau)$ curve computed from the "true" phases $\phi_H = \arg(A)$. We also show here the theoretical curve according to the Eq. (17); it demonstrates a very good correspondence with the numerical results for the "true" phases. In order to obtain the theoretical curve, we write the phase equation for the system (18) and in this way find the effective parameters—namely, the noise intensity and coupling strength—for the Eq. (17); here we use $\Delta t = h$. Note also that for the phases obtained via the Hilbert transform, the effective noise appears to be larger. This occurs due to the property of the transform that "transfers" some components of the amplitude noise to the phases; as a result, the Hilbert phases are in this example more noisy than the "true" phases. The right panel of Fig. 1 shows the synchronization index and the cross-correlation function of $\mathrm{Re}(A_1)$ and $\mathrm{Re}(A_2)$, which are in correspondence with our theoretical considerations. Concerning the impact of the time interval Δt,[3] we mention that the curves $\mathcal{E}(\tau)$, computed for different Δt, comply with Eq. (17) and its discussion. In the presentation of the error in the normalized form, $\mathcal{E}_N(\tau)$, the increase of Δt results in a more pronounced minimum.

As a next example we consider unidirectionally coupled chaotic Rössler oscillators. It is known that the phase dynamics of this system is qualitatively similar to that of noisy limit cycle oscillators: the phase exhibits a random-walk-like motion, though the diffusion coefficient is relatively small [24,29]. Therefore, we expect that our approach can be applied to the systems of this class as well. The model we simulate reads

$$\dot{x}_1 = -\omega_1 y_1 - z_1 + \varepsilon x_2(t - T), \quad \dot{x}_2 = -\omega_2 y_2 - z_2,$$
$$\dot{y}_1 = \omega_1 x_1 + 0.15 y_1, \quad \dot{y}_2 = \omega_2 x_2 + 0.15 y_2,$$
$$\dot{z}_1 = 0.2 + z_1(x_1 - 10), \quad \dot{z}_2 = 0.2 + z_2(x_2 - 10), \tag{19}$$

where $\omega_{1,2} = 0.99 \pm 0.08$ are the natural frequencies of the oscillators, ε is the coupling strength, and T denotes the delay in coupling. Numerical solutions of Eqs. (19) have been obtained by means of a predictor-corrector integration scheme with a fixed step $h = 2\pi/100$. The results for $\varepsilon = 0.05$ and $T = 3200h \approx 202$ are presented in Fig. 2 for $\Delta t = 20h$. Here we also show the envelope of the cross-correlation function between x_1 and x_2; note that in this case it is not close to the $\rho(\tau)$ curve due to uncorrelated fluctuations of chaotic amplitudes. Results of further simulations (not shown here) demonstrate that (i) the delay can be correctly estimated also in case of a relatively strong coupling $\varepsilon = 0.4$, when the phase dynamics approximation is quite poor, and (ii) good estimates can be obtained even with large Δt of the order of the oscillation period.

We conclude the discussion of the unidirectional coupling case by emphasizing that in a practical situation we do not have to know beforehand which system is the driver. Indeed, we shall consequently fit two dependences, $\phi_1(t + \Delta t)$

[3] In these as well as in the following computations the integration step is kept small ($h = 2\pi/100$ in this example) and then the data points are downsampled to increase Δt.

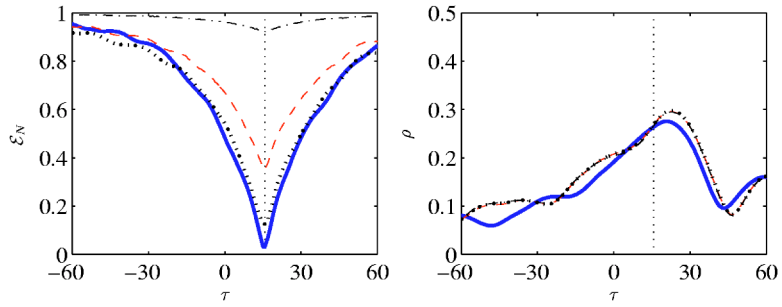

FIG. 3. (Color online) Unidirectional delayed coupling of noisy limit cycle oscillators [Eqs. (18)]. The value of the delay in coupling is revealed from the dependences of the fitting error $\mathcal{E}_N$ and synchronization index ρ versus shift τ between the two time series of phases (left and right panels, respectively). The dotted vertical lines mark the true value of the delay T. Bold (blue) line illustrates the case of the noisy driver and noise-free driven system; dashed (red) line corresponds to the case when the response system is noisy as well. Dot-dashed line (black) shows the results for the case when both systems are noisy and the observed signals are contaminated by observational noises. Finally, the dotted (black) line shows the results for the latter case obtained after smoothing the signals as described in the text; the fact that the curves obtained after smoothing nearly coincide with the curves for noise-free response system demonstrates that the delay can be efficiently estimated from real-world data. (In the right panel three of four curves nearly coincide.) Note that $\rho(\tau)$ dependence provides a biased estimate of the delay.

$-\phi_1(t)$ on $\phi_1(t)$, $\phi_2(t-\tau)$ and $\phi_2(t+\Delta t)-\phi_2(t)$ on $\phi_2(t)$, $\phi_1(t-\tau)$, and look which one exhibits a minimum.

B. Performance of the delay estimation and the influence of parameters

1. Observational noise

In this section we explore the effects of intrinsic and/or measurement noise on the performance of the two time delay estimators MFE and SIE. For this purpose, we again consider the system(18); see Fig. 3. First we compare the results for the case of noise-free ($\sqrt{2D_1}=0$) and noisy ($\sqrt{2D_1}=0.05$) driven systems (bold blue and dashed red lines, respectively); the noise in the driver was $\sqrt{2D_2}=0.3$. As expected, we see that noise in the driven system reduced the performance of the delay estimation, making the minimum of the curve less pronounced. Next, we add observational white Gaussian noise $\zeta_{1,2}$ with rms value $\sqrt{2D_{1,2}^{obs}}=0.1$ to the signals $\mathrm{Re}\{A_{1,2}\}$. That means that the phases has been computed by means of the Hilbert transform from $x_{1,2}^{obs}=\mathrm{Re}\{A_{1,2}(t)\}+\zeta_{1,2}(t)$. The results for the case when both internal and observational noises are present are shown by the dot-dashed line (black). Then, as is typically done in the processing of real-world data, the noisy signals have been smoothed using a Savitzky-Golay fourth-order polynomial filter and subsequently their phases have been extracted by means of the Hilbert transform; the corresponding results are shown by the dotted (black) line. The results of this example have been obtained by setting $\Delta t=10h$. Note that for better comparison of different curves we use here the normalized error.

Concluding this example, we note that (i) observational (and to some extent intrinsic) noise can be easily filtered out and therefore does not hamper the delay estimation; (ii) intrinsic noise in the driven systems reduces the sensitivity of both algorithms to the presence of a delay; however, this does not bias the MFE; and (iii) we recall that estimation is possible only due to phase diffusion in the driver.

2. Influence of noise and coupling strength

In order to illustrate further the performance of the methods and systematically analyze the influence of the noise intensity, coupling strength, and other parameters, we exploit a computationally efficient model; namely, we consider two unidirectionally coupled noisy sine maps:

$$\phi_1(n+1)=\phi_1(n)+\omega_1+\varepsilon\sin[\phi_2(n-T)-\phi_1(n)]+\xi_1(n),$$
$$\phi_2(n+1)=\phi_2(n)+\omega_2+\xi_2(n), \tag{20}$$

where modulo 2π operation is applied at every iteration and the parameters $\omega_{1,2}$, ε, and T denote the natural frequencies, coupling strength, and delay, respectively. In the following simulations, we set $\omega_{1,2}=0.511\mp\Delta\omega$.

Figure 4 shows the effect of coupling strength on the per-

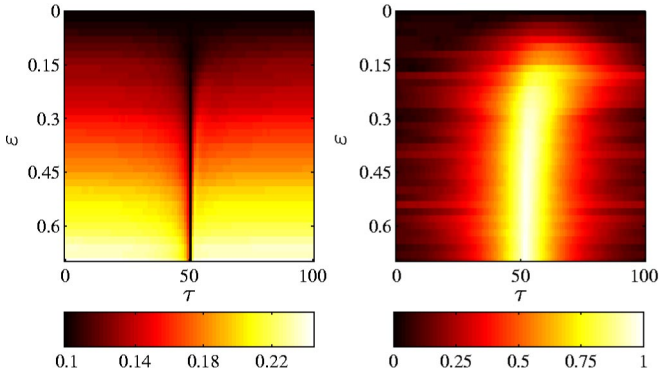

FIG. 4. (Color online) The influence of the driving strength on the estimation of delay by means of the MFE (left panel) and SIE (right panel) algorithms for unidirectionally coupled noisy maps [Eq. (20)]. Gray scales (colors) code the values of the fitting error $\mathcal{E}(\tau)$ and synchronization index $\rho(\tau)$, respectively. Note that the MFE algorithm provides accurate estimates of the delay as long as the driving strength ε exceeds the noise level in the driven system [cf. Eq. (16)]. The SIE algorithm produces a biased estimate, in accordance with Eq. (13).

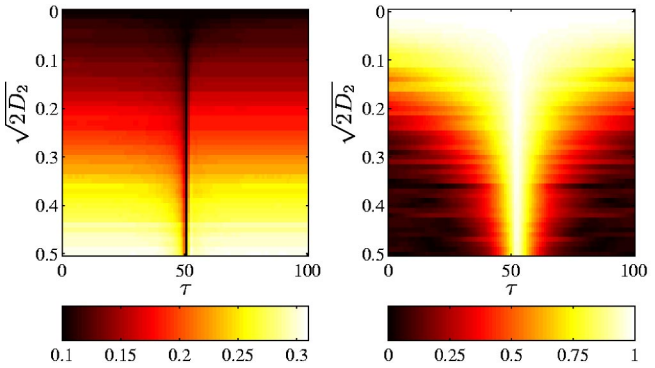

FIG. 5. (Color online) The influence of the noise intensity in the driver on the estimation of delay by means of the MFE (left panel) and SIE (right panel) algorithms for unidirectionally coupled noisy maps [Eq. (20)]. Note that the noise facilitates the identification of delay.

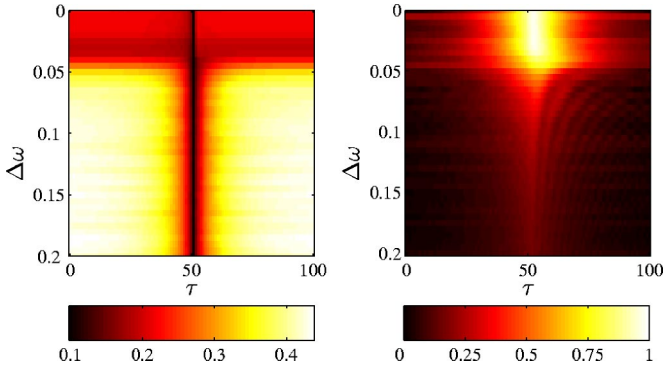

FIG. 6. (Color online) The influence of detuning on the estimation of delay by means of the MFE (left panel) and SIE (right panel) algorithms for unidirectionally coupled noisy maps [Eq. (20)]. Note that with an increase of the detuning, the SIE algorithm fails, while the MFE algorithm provides the correct estimate in the whole range of the detuning.

formance of the methods MFE and SIE. Here the parameters are $T=50$, $\Delta\omega=0.01$, $\sqrt{2D_1}=0.1$, and $\sqrt{2D_2}=0.3$, whereas the coupling strength ε is varied. In a similar way we depict the effect of the noise intensity in Fig. 5, for $T=50$, $\Delta\omega=0.01$, $\varepsilon=0.6$, and $\sqrt{2D_1}=0.1$, whereas the intensity of the noise in the driver D_2 is varied. In agreement with the theoretical predictions, both methods allow the identification of delay as long as the driving is sufficiently strong. The delay is accurately recovered by the MFE algorithm, while biased estimates [cf. Eq. (13)] are obtained by means of the SIE algorithm. Furthermore, the presence of noise in the driver system is essential for the detection and estimation of delay. With an increase of the noise intensity, the minimum of $\mathcal{E}(\tau)$ and maximum of $\rho(\tau)$ appear and become more pronounced.

3. Influence of the detuning

In this section we consider the effect of the detuning parameter $\Delta\omega$. Its variations result in a qualitative change of the dynamics (synchronous versus quasiperiodic) and we cannot exactly predict the effect of this parameter from our theoretical considerations. The results are shown in Fig. 6 for the following parameters: $T=50$, $\varepsilon=0.6$, $\sqrt{2D_1}=0.1$, and $\sqrt{2D_2}=0.3$; they provide two interesting observations. First, the identification of delay is possible even for zero detuning, provided that the driver is noisy and the driving strength is sufficiently large to overcome the intrinsic noise in the response system. Within these limits, the MFE algorithm becomes less sensitive to the detuning effect, while the SIE algorithm gradually loses its performance with an increase of the detuning. Second, far from the synchronization, $\rho(\tau)$ is small and a reliable identification of a global maximum becomes problematic. On the contrary, the MFE algorithm provides a clearly defined minimum for the whole range of the detuning.

A final remark concerns the data requirements of the algorithms. In all the examples given here we use 5000 periods of data for the continuous-time models and 10 000 iterations for the discrete maps. Preliminary computations show that reasonable results can be obtained from short (of the order of hundreds of periods) data sets as well and that the MFE algorithm is less demanding than the SIE algorithm.

C. Bidirectional coupling

In this section we consider bidirectionally coupled systems. As the model example we take noisy van der Pol oscillators

$$\begin{aligned}\ddot{x}_1 - 0.1(1-x_1^2)\dot{x}_1 + \omega_1^2 x_1 + \xi_1 &= \varepsilon_1[\dot{x}_2(t-T_{12}) - \dot{x}_1(t)],\\ \ddot{x}_2 - 0.1(1-x_2^2)\dot{x}_2 + \omega_2^2 x_2 + \xi_2 &= \varepsilon_2[\dot{x}_1(t-T_{21}) - \dot{x}_2(t)],\end{aligned} \tag{21}$$

The interaction is characterized by two delays that are generally different. In the simulation we take $T_{12}=2800h \approx 176$ and $T_{21}=4300h \approx 270$. The other parameter values are $\varepsilon_1=0.4$, $\varepsilon_2=0.2$, $\sqrt{2D_{1,2}}=0.3$, and $\omega_{1,2}^2=1\pm0.2$. Now we have to compute two fitting errors $\mathcal{E}_{12}$ and $\mathcal{E}_{21}$, fitting, respectively, the first or second phase increment in the same way as for the unidirectional coupling. The results are shown in Fig. 7. We see that both $\mathcal{E}(\tau)$ and $\rho(\tau)$ dependences exhibit mul-

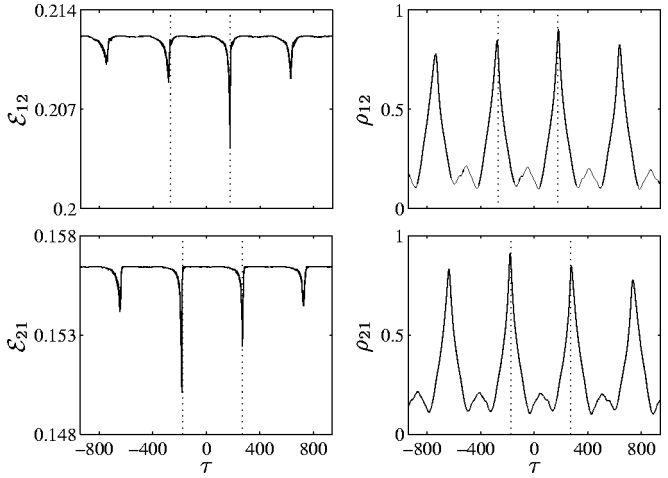

FIG. 7. Bidirectional delayed coupling of Van der Pol oscillators [Eqs. (19)]. The dotted vertical lines mark the true value of the delays T_{12} and T_{21}.

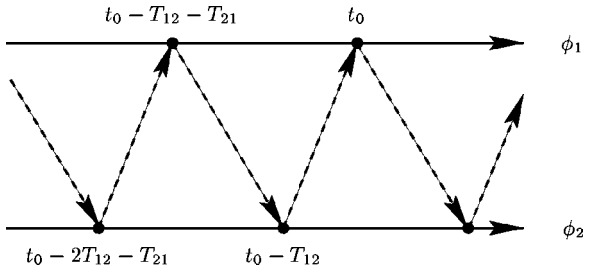

FIG. 8. Schematic illustration of the correlation between time series $\phi_{1,2}$. Phase $\phi_1(t_0)$ is tightly correlated with $\phi_2(t_0-T_{12})$. Therefore, quantification of the interrelation between the shifted phases provides an extremum for shift $\tau=T_{12}$. On the other hand, $\phi_1(t_0)$ is tightly correlated with $\phi_2(t_0-2T_{12}-T_{21})$, and hence, the shift $\tau=T_{12}+(T_{12}+T_{21})$ also provides an extremum.

tiple extrema. This can be understood in the following way. The phase of the first signal at a certain time instant $\phi_1(t)$ is strongly correlated with $\phi_2(t-T_{12})$, and therefore the shift $\tau=T_{12}$ provides an extremum in the $E(\tau)$ and $\rho(\tau)$ dependences. On the other hand, $\phi_2(t-T_{12})$ is strongly correlated with $\phi_1(t-T_{12}-T_{21})$, and $\phi_1(t-T_{12}-T_{21})$ is correlated with $\phi_2(t-2T_{12}-T_{21})$; see Fig. 8. Hence, the extrema of $\mathcal{E}_{12}(\tau)$, $\rho_{12}(\tau)$ are found at shifts $\tau=T_{12}+n(T_{12}+T_{21})$, $n=0,1,2,\ldots$. Similar considerations for the second signal and the negative shifts explain the appearance of a series of peaks at the delay estimation in bidirectionally coupled systems. Noteworthy, the delays can be estimated for zero detuning between the oscillators as well. Note also that different minimal values of $\mathcal{E}_{12}(\tau)$ and $\mathcal{E}_{21}(\tau)$ reflect the asymmetry in the coupling and in the noise intensities.

D. Multiple delays

Generally speaking, an interaction between two systems can function over several pathways, each having its own delay. In this case our basic model (1) should be extended by several additional terms. The systematic analysis of such a complicated interaction is beyond the framework of this paper; in the following example we just show that in principle the model fitting technique can be used in this case as well. For this purpose we consider unidirectionally coupled systems with multiple delays:

$$\dot{A}_1(t) = (1 + i\omega_1)A_1(t) - |A_1(t)|^2 A_1(t) - \sum_{k=1}^{3} \varepsilon_k A_2(t - T_k) + \xi_1(t),$$
$$\dot{A}_2(t) = (1 + i\omega_2)A_2(t) - |A_2(t)|^2 A_2(t) + \xi_2(t). \tag{22}$$

The parameters are $\omega_{1,2}=1\pm0.1$, $\sqrt{2D_1}=0.1$, $\sqrt{2D_2}=0.3$, $\varepsilon_1=0.3$, $\varepsilon_2=0.15$, $\varepsilon_3=0.1$, $T_1=170h\approx10.7$, $T_1=380h\approx23.9$, and $T_1=600h\approx37.7$. The results, presented in Fig. 9, suggest that the MFE algorithm is effective in this case as well. Indeed, the $\mathcal{E}_N(\tau)$ dependence exhibits three minima, and at least the delay in the dominating, strongest, driving term can be correctly identified. The second and third minima provide biased estimates. On the contrary, the SIE approach, as well as the cross-correlation analysis, cannot distinguish whether single or multiple delays are present.

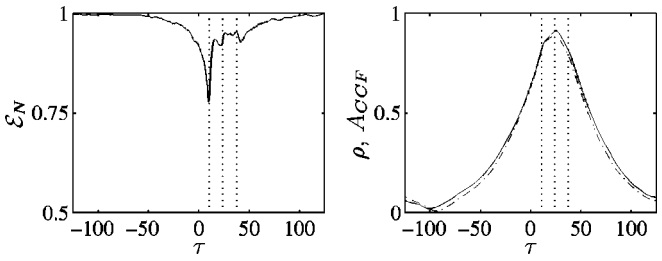

FIG. 9. Unidirectional driving with multiple delays [Eqs. (22)]. The dashed line in the right panels shows the envelope of the cross-correlation function. Note that the MFE approach correctly indicates the number of delayed interactions.

V. DISCUSSION

In this paper we have shown that the delay in weak coupling between two oscillators can be estimated from the time series, provided these series are suitable for the computation of instantaneous phases. We emphasize that if the signals under study come from coupled self-sustained oscillators, then the determination of the delay is not possible from the measurements of the phase difference. Indeed, the latter is not determined solely by the delay, but depends also on the other parameters of interacting systems. Concerning the use of the standard tool of data analysis—the correlation function—we underline that an estimate of the delay can be obtained by analysis of the envelope of the function, but not from the position of its maxima (the latter are related to the phase shift between the signals). Last but not least, in the case of oscillators which are close to synchrony, the envelope of the cross-correlation function provides a systematically overestimated value of the delay. It is important that delay estimation by means of the model fitting can be easily combined with the estimation of the directionality of coupling [30–34]. We conclude the presentation of the two presented techniques for delay estimation by a discussion of several important points.

a. *The role of noise and chaos.* We emphasize that estimation of the delay is possible only if the driving system is noisy and/or chaotic, so that its phase is diffusive, $D_2>0$ (for definiteness, we discuss now the delay in driving from system 2 to system 1). Indeed, the dependences of both synchronization index and of the error of the fit on τ [Eqs. (12) and (17)] have the form $\sim e^{-D_2|\tau-T|}$. The maximum of $\rho(\tau)$ or minimum of $E(\tau)$ is well defined only if D_2 is sufficiently large. The physical meaning of this condition is clear: if there is no diffusion of the phase ϕ_2, then the values of ϕ_2 at different instants of time are completely correlated, and one cannot determine at which time instant t' the phase $\phi_2(t')$ affects the dynamics of $\phi_1(t)$. Mathematically, this would mean that the effect of delay is reduced to changing the constant α in the first of Eqs. (2), $\alpha\to\alpha+\omega_2\tau$. Only when the phase ϕ_2 performs a random walk can we determine at which time instant it influences the phase ϕ_1. Certainly, the same considerations are valid for the determination of the delay in driving in the reverse direction—i.e., from system 1 to system 2.

b. *Complementary applicability of the methods.* Com-

paring the two presented techniques we note that the method based on the synchronization index is most efficient if two systems are close to synchrony, whereas the method based on the model fitting does not have this limitation. As the advantage of the first method we mention the absence of parameters and simplicity of implementation; on the other hand, it provides a biased estimate. For delays of the order of the oscillation period this bias may be not negligible. Generally, we suggest that the two methods should be used in a complementary way.

c. *Limitations.* Application of the method to real data requires an assumption that the underlying systems can be (at least approximately) modeled by phase equations (1). Although the preliminary computations demonstrate that the technique can be effective in more complex cases—e.g., with multiple delays—this limitation should be taken into account. In particular, the presence of internal delays requires an additional treatment.

ACKNOWLEDGMENTS

The work has been supported by DFG (SFB 555 "Complex nonlinear processes") and IKYDA-DAAD bilateral German-Greek exchange Program. L.C. aknowledges partial financial support from the Research Committee of Patras University (Karatheodori Research Project No. 2459). We thank Tassos Bountis for fruitful discussions.

APPENDIX A: ANALYTIC CALCULATION OF THE SYNCHRONIZATION INDEX

Here we present a statistical analysis of Eq. (10). Integrating it, we obtain

$$\Psi = \int_{-\infty}^{t} [\xi_1(u) - \xi_2(u-T)]e^{(u-t)A}du.$$

Let us find the variance of our observable:

$$\begin{aligned}\mathrm{Var}(\theta) &= \mathrm{Var}(\Psi + (T-\tau)\omega_2 + \psi_0 + \eta) \\ &= \mathrm{Var}(\Psi + \eta) \\ &= \langle\Psi^2\rangle + \left\langle \left(\int_{t-\tau}^{t-T} \xi_2(u)du \right)^2 \right\rangle + 2\langle \Psi \int_{t-\tau}^{t-T} \xi_2(u)du \rangle,\end{aligned} \tag{A1}$$

where we use that $\langle\Psi\rangle = \langle\eta\rangle = 0$ and $(T-\tau)\omega_2 + \psi_0 = \text{const}$, as well as the definition of η given by Eq. (8). Because $\Psi(t)$ depends only on the values of $\xi_2(s)$ for $-\infty < s < t-T$ and η depends only on the values of $\xi_2(s)$ for s lying in the interval between $t-\tau$ and $t-T$, we conclude that for $\tau < T$ these quantities are independent and the last term vanishes. Thus, for $\tau < T$, Eq. (9) holds.

For $\tau > T$ we compute separately all three terms in Eq. (A1). For the first we get

$$\begin{aligned}\langle\Psi^2\rangle &= \left\langle \int_{-\infty}^{t} [\xi_1(s) - \xi_2(s-T)]e^{(s-t)A}ds \int_{-\infty}^{t} [\xi_1(u) - \xi_2(u-T)]e^{(u-t)A}du \right\rangle \\ &= 2(D_1 + D_2)\int_{-\infty}^{t} e^{(x-t)A}dx \\ &= \frac{2(D_1 + D_2)}{A}.\end{aligned} \tag{A2}$$

The second term gives

$$\left\langle \int_{t-\tau}^{t-T} \xi_2(u)du \int_{t-\tau}^{t-T} \xi_2(s)ds \right\rangle = 2D_2|\tau - T|.$$

The third term gives

$$\begin{aligned}2\left\langle \Psi \int_{t-\tau}^{t-T} \xi_2(u)du \right\rangle &= 2\int_{-\infty}^{t} ds \int_{t-\tau}^{t-T} \\ &\quad \times du\langle[\xi_1(s) - \xi_2(s-T)]\xi_2(u)\rangle e^{(s-t)A} \\ &= -4D_2\int_{t-\tau}^{t-T} e^{(u+T-t)A}du \\ &= -\frac{4D_2}{A}(1 - e^{(T-\tau)A}).\end{aligned} \tag{A3}$$

Finally, for all τ we obtain

$$\mathrm{Var}(\theta) = \begin{cases} \dfrac{2(D_1 + D_2)}{A} + 2D_2(\tau - T) - \dfrac{4D_2}{A}(1 - e^{-(\tau-T)A}), \\ \qquad \tau \geqslant T, \\ \dfrac{2(D_1 + D_2)}{A} - 2D_2(\tau - T), \\ \qquad \tau < T. \end{cases} \tag{A4}$$

Because the distributions of Ψ and η are Gaussian, the synchronization index is related to this value as $\rho(\tau) = \exp[-\mathrm{Var}(\theta)/2]$, which gives formula (12).

APPENDIX B: ANALYTIC CALCULATION OF THE FITTING ERROR

Here we present the derivation of the expressions for the error of the fit for the model (2). The test function is given by Eq. (15). As the second phase at time $t-\tau$ can be represented as $\phi_2(t-\tau) = \phi_2(t-T) + \eta + \omega_2(T-\tau)$, where $\eta = \int_{t-\tau}^{t-T} \xi_2 dt$ is a Gaussian process with the variance $2D_2|T-\tau|$, the test function can be rewritten as

$$f'(t) = \omega' - \varepsilon' \sin(\psi - \eta + \alpha').$$

The constants ω', ε', and $\alpha' = \tilde{\alpha}' - \omega_2(T-\tau)$ should be found by a least-mean-squares fitting procedure—i.e., by minimizing

$$E^2 = \langle [f(t) - f'(t)]^2 \rangle$$
$$= \langle [\omega_1 - \omega' - \varepsilon \sin(\psi + \alpha) + \varepsilon' \sin(\psi - \eta + \alpha') + \xi_1(t)]^2 \rangle.$$

We can complete analytic computations in two limit cases.

In the first case we assume that the systems are in a quasiperiodic state. It means that the phase difference ψ [see Eq. (5)] grows with time and the distribution of $\psi \, mod \, 2\pi$ can be approximated by a uniform one. Performing squaring on the RHS we obtain

$$\begin{aligned}[f(t) - f'(t)]^2 = {} & \omega_1^2 + \omega'^2 + \varepsilon^2 \sin^2(\psi + \alpha) \\ & + \varepsilon'^2 \sin^2(\psi - \eta + \alpha') + \xi_1^2 - 2\omega_1\omega' \\ & - 2\omega_1\varepsilon \sin(\psi + \alpha) + 2\omega_1\varepsilon' \sin(\psi - \eta + \alpha') \\ & + 2\omega_1\xi_1 + 2\omega'\varepsilon \sin(\psi + \alpha) \\ & - 2\omega'\varepsilon' \sin(\psi - \eta + \alpha') - 2\omega'\xi_1 \\ & - 2\varepsilon\varepsilon' \sin(\psi + \alpha)\sin(\psi - \eta + \alpha') \\ & - 2\varepsilon \sin(\psi + \alpha)\xi_1 + 2\varepsilon' \sin(\psi - \eta + \alpha')\xi_1.\end{aligned}$$

To compute the least mean approximation error E, we have to average this expression. We perform this neglecting the correlations between ϕ_1 and ϕ_2, which is justified for the considered far from synchrony case. The averaging includes the integration

$$(2\pi)^{-2} \int \int_0^{2\pi} [f(t) - f'(t)]^2 d\phi_2 d\phi_1$$

and the averaging over the distribution of the noise. The terms with ξ_1 and the terms with sine-function vanish, whereas the terms $\sin^2(\cdot)$ give $1/2$. As a result we obtain

$$\begin{aligned}E^2 = {} & \omega_1^2 + \omega'^2 + \varepsilon^2/2 + \varepsilon'^2/2 + \langle \xi_1^2 \rangle - 2\omega_1\omega' \\ & - 2\varepsilon\varepsilon' \langle \sin(\psi + \alpha)\sin(\psi - \eta + \alpha') \rangle.\end{aligned}$$

The last term gives

$$\begin{aligned}& \varepsilon\varepsilon' \langle \cos(2\psi - \eta + \alpha + \alpha') - \cos(\alpha + \eta - \alpha') \rangle \\ & = -\varepsilon\varepsilon' \langle \cos(\alpha + \eta - \alpha') \rangle \\ & = -\varepsilon\varepsilon' [\langle \cos\eta \rangle \cos(\alpha - \alpha') - \langle \sin\eta \rangle \sin(\alpha - \alpha')].\end{aligned}$$

With $\langle \cos\eta \rangle = \exp(-D_2|T-\tau|)$ and $\langle \sin\eta \rangle = 0$ we finally obtain

$$\begin{aligned}E^2 = {} & \omega_1^2 + \omega'^2 + \varepsilon^2/2 + \varepsilon'^2/2 + \langle \xi_1^2 \rangle - 2\omega_1\omega' \\ & - \varepsilon\varepsilon' \exp(-D_2|T - \tau|)\cos(\alpha - \alpha').\end{aligned}$$

The optimal value of the parameters ω', α', and ε' can be obtained from the following conditions:

$$\frac{\partial E}{\partial \omega'} = 0, \quad \frac{\partial E}{\partial \alpha'} = 0, \quad \frac{\partial E}{\partial \varepsilon'} = 0,$$

which yields $\omega' = \omega_1$, $\alpha = \alpha'$, and $\varepsilon' = \varepsilon \exp(-D_2|T-\tau|)$. Thus, the error at the best fit is

$$\begin{aligned}E^2(\tau) &= \frac{\varepsilon^2}{2} + \frac{\varepsilon^2}{2} e^{-2D_2|T-\tau|} - \varepsilon^2 e^{-2D_2|T-\tau|} + \langle \xi_1^2 \rangle \\ &= \frac{\varepsilon^2}{2}(1 - e^{-2D_2|T-\tau|}) + \langle \xi_1^2 \rangle. \qquad \text{(B1)}\end{aligned}$$

Now we consider another limit case where we assume that the systems are close to synchrony and the fluctuations around the constant value of the phase difference $\Psi = \psi - \arcsin(\nu/\varepsilon) + \alpha$ are small [cf. Eq. (10) and its discussion]. We rewrite the RHS of Eq. (2) in the following form [cf. Eq. (14)] :

$$\begin{aligned}f(\phi_1(t), \phi_2(t - T)) &= \omega_1 - \varepsilon \sin(\psi + \alpha) + \xi_1(t) \\ &= \omega_1 - \varepsilon \sin[\Psi + \arcsin(\nu/\varepsilon)] + \xi_1(t).\end{aligned}$$

Using the smallness of Ψ and the notation introduced by Eq. (11) we obtain

$$f(t) = \omega_1 - \nu - \varepsilon\sqrt{1 - \nu^2/\varepsilon^2}\Psi + \xi_1(t) = b - A\Psi + \xi_1(t),$$

where $b = \omega_1 - \nu$. Our test function is

$$f'(t) = b' - A'(\Psi + \eta).$$

The least-mean-squares error of the fit is then

$$E^2 = \langle [f(t) - f'(t)]^2 \rangle = \langle (b - A\Psi + \xi_1 - b' + A'\Psi + A'\eta)^2 \rangle.$$

Squaring the RHS and using $\langle \Psi \rangle = \langle \eta \rangle = \langle \xi_1 \rangle = 0$ we obtain

$$\begin{aligned}E^2 = {} & (b - b')^2 + (A - A')^2 \langle \Psi^2 \rangle + (A')^2 \langle \eta^2 \rangle \\ & - 2A'(A - A') \langle \Psi\eta \rangle + \langle \xi_1^2 \rangle.\end{aligned}$$

The conditions

$$\frac{\partial E}{\partial b'} = 0, \quad \frac{\partial E}{\partial A'} = 0,$$

provide the optimal values $b' = b$ and $A' = A$ $(\langle \Psi^2 \rangle + \langle \Psi\eta \rangle)/\langle (\Psi + \eta)^2 \rangle$. With these values we obtain, for the error,

$$E^2(\tau) = A^2 \left(\langle \Psi^2 \rangle - \frac{(\langle \Psi^2 \rangle + \langle \Psi\eta \rangle)^2}{\langle (\Psi + \eta)^2 \rangle} \right) + \langle \xi_1^2 \rangle, \qquad \text{(B2)}$$

where the terms $\langle \Psi^2 \rangle$, $\langle \Psi\eta \rangle$, and $\langle (\Psi + \eta)^2 \rangle$ are given by Eqs. (A2) and (A3), and (A4), respectively. This result is illustrated in Fig. 10 for the parameters $D_1 = 0.1$, $D_2 = 0.1$, $T = 50$, $\varepsilon = 0.05$, and $\nu = 0.01$.

APPENDIX C: FOURIER-BASED MODEL SELECTION

Here we discuss the choice of the test function for the model fitting estimate of delay. The first question which arises in the implementation of the MFE algorithm is related to the determination of the particular terms in the double Fourier series that approximates $\Delta\phi_1$ or $\Delta\phi_2$. The choice of the harmonics depends on the balance between reducing computational cost and ensuring numerical stability and quality of the fit from the limited amount of data. Practically, the identification of dominant terms of the coupling function can be done by means of the two-dimensional discrete Fou-

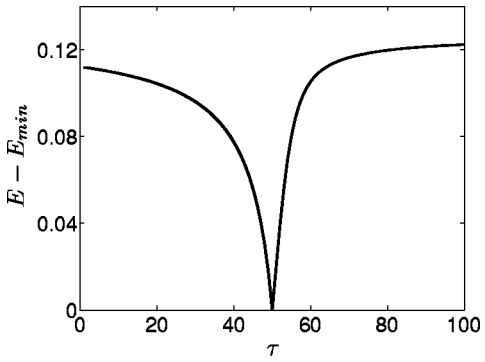

FIG. 10. The theoretical dependence of the error of the optimal fit on the shift between the time series of phases [see Eq. (B2)]. The position of the minimum of the error coincides with the true value of the delay $T=50$. The value of the minimum is determined by the noise level in the driven system.

rier transform of $\Delta\phi(\phi_1,\phi_2)$ over the $[0,2\pi)\times[0,2\pi)$ plane:

$$F(k_1,k_2)=\frac{1}{NM}\sum_{0}^{N-1}\sum_{0}^{M-1}\Delta\phi(\phi_1,\phi_2)e^{i(k_1\phi_1+k_2\phi_2)}, \quad \text{(C1)}$$

where $k_{1,2}$ denote the spatial frequencies along the ϕ_1 and ϕ_2 coordinates, respectively. (Here the phases are taken modulo 2π.) The points $\Delta\phi(\phi_1,\phi_2)$ are not regularly distributed in the phase plane. Therefore, in order to make use of the fast algorithm for the two-dimensional Fourier transform, we perform the Delaunay-triangulation-based cubic interpolation on a uniform grid on the square $[0,2\pi)\times[0,2\pi)$ with the grid step $2\pi/100$. The Nyquist theorem provides the upper limit of the frequencies resolved by these data, $k_1^{max}=k_2^{max}=50$, which, under assumption that the coupling functions in Eqs. (1) are smooth, can be considered as sufficiently large to prevent aliasing.

The next step is the choice of the significant Fourier coefficients. For this purpose we perform a surrogate data test.

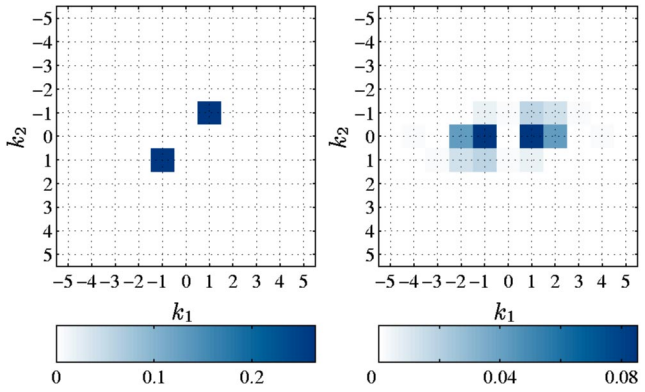

FIG. 11. (Color online) Two-dimensional discrete Fourier transform $F^2(k_1,k_2)$ of the phase increment $\Delta\phi_1=\Delta\phi_1(\phi_1,\phi_2)$ for two unidirectionally coupled Stuart-Landau (left panel) or Rössler (right panel) oscillators [see Eqs. (18) and (19)]. Gray scales (colors) code the magnitude of the (significant) Fourier coefficients. Only the first ten harmonics are shown.

Namely, we compute the Fourier coefficients $\tilde{F}(k_1,k_2)$ for 100 realizations of the randomly shuffled $\Delta\phi$ and take $\langle\max(\tilde{F}^2(k_1,k_2))\rangle$ as the threshold value, where $\langle\rangle$ means averaging over the realizations of surrogates. It means that for the model fitting we use only the terms (k_1,k_2) which satisfy $F^2(k_1,k_2)\geqslant\max(\tilde{F}^2(k_1,k_2))$. An example of this analysis is given in Fig. 11. In particular, we can see that the modeling of the chaotic system requires essentially more terms than the modeling of the simple limit cycle oscillator.

Note that the presented approach is feasible only when noise in the otherwise synchronous oscillators or quasiperiodic dynamics ensure a quite uniform scattering of phase points over the $[0,2\pi)\times[0,2\pi)$ square. The described Fourier-based model selection could be also exploited for an estimation of the directionality of coupling [30–34] that requires model fitting by Fourier series as well. For a general discussion of nonparametric model reconstruction see, e.g., [35–38].

[1] E. Niebur, H. G. Schuster, and D. M. Kammen, Phys. Rev. Lett. **67**, 2753 (1991).
[2] D. V. Ramana Reddy, A. Sen, and G. L. Johnston, Phys. Rev. Lett. **80**, 5109 (1998).
[3] M. K. S. Yeung and S. H. Strogatz, Phys. Rev. Lett. **82**, 648 (1999).
[4] D. V. Ramana Reddy, A. Sen, and G. L. Johnston, Physica D **129**, 15 (1999).
[5] D. V. Ramana Reddy, A. Sen, and G. L. Johnston, Physica D **144**, 335 (2000).
[6] D. V. Ramana Reddy, A. Sen, and G. L. Johnston, Phys. Rev. Lett. **85**, 3381 (2000).
[7] T. Heil *et al.*, Phys. Rev. Lett. **86**, 795 (2001).
[8] A. Takamatsu, T. Fujii, and I. Endo, Phys. Rev. Lett. **85**, 2026 (2000).
[9] C. Keyl *et al.*, Clin. Sci. **99**, 113 (2000).
[10] W. Gerstner, Phys. Rev. Lett. **76**, 1755 (1996).
[11] N. Brunel and V. Hakim, Neural Comput. **11**, 1621 (1999).
[12] D. Golomb, D. Hansel, and G. Mato, in *Neuro-informatics and Neural Modeling*, Vol. 4 of *Handbook of Biological Physics*, edited by F. Moss and S. Gielen (Elsevier, Amsterdam, 2001), pp. 887–968.
[13] M. J. Bünner *et al.*, in *Nonlinear Physics of Complex Systems. Current Status and Future Trends*, edited by J. Parisi, S. C. Müller, and W. Zimmermann (Springer-Verlag, Berlin, 1996), pp. 229–238.
[14] M. J. Bünner, T. Meyer, A. Kittel, and J. Parisi, Phys. Rev. E **56**, 5083 (1997).
[15] H. Voss and J. Kurths, Phys. Lett. A **234**, 336 (1997).
[16] R. Hegger, M. J. Bünner, H. Kantz, and A. Giaquinta, Phys.

Rev. Lett. **81**, 558 (1998).
[17] M. J. Bünner *et al.*, Europhys. Lett. **42**, 353 (1998).
[18] M. J. Bünner *et al.*, Eur. Phys. J. D **10**, 165 (2000).
[19] M. J. Bünner *et al.*, Eur. Phys. J. D **10**, 177 (2000).
[20] B. P. Bezruchko, A. S. Karavaev, V. I. Ponomarenko, and M. D. Prokhorov, Phys. Rev. E **64**, 056216 (2001).
[21] W. Horbelt, H. U. Voss, and J. Timmer, Phys. Lett. A **299**, 513 (2002).
[22] T. Ohira and R. Sawatari, Phys. Rev. E **55**, R2077 (1997).
[23] M. G. Rosenblum *et al.*, in *Neuro-informatics and Neural Modeling*, Vol. 4 of *Handbook of Biological Physics*, edited by F. Moss and S. Gielen (Elsevier, Amsterdam, 2001), pp. 279–321.
[24] A. Pikovsky, M. Rosenblum, and J. Kurths, *Synchronization: A Universal Concept in Nonlinear Sciences* (Cambridge University Press, Cambridge, England, 2001).
[25] Y. Kuramoto, *Chemical Oscillations, Waves and Turbulence* (Springer, Berlin, 1984).
[26] D. Rybski, S. Havlin, and A. Bunde, Physica A **320**, 601 (2003).
[27] E. Rodriguez *et al.*, Nature (London) **397**, 430 (1999).
[28] R. L. Stratonovich, *Topics in the Theory of Random Noise* (Gordon and Breach, New York, 1963).
[29] A. Pikovsky, M. Rosenblum, G. Osipov, and J. Kurths, Physica D **104**, 219 (1997).
[30] M. Rosenblum and A. Pikovsky, Phys. Rev. E **64**, 045202(R) (2001).
[31] M. G. Rosenblum *et al.*, Phys. Rev. E **65**, 041909 (2002).
[32] B. P. Bezruchko, V. Ponomarenko, A. S. Pikovsky, and M. G. Rosenblum, Chaos **13**, 179 (2003).
[33] R. Mrowka, L. Cimponeriu, A. Patzak, and M. Rosenblum, Am. J. Physiol. **285**, R1395 (2003).
[34] D. A. Smirnov and B. P. Bezruchko, Phys. Rev. E **68**, 046209 (2003).
[35] K. Judd and A. Mees, Physica D **82**, 426 (1995).
[36] L. A. Aguirre, U. S. Freitas, C. Letellier, and J. Maquet, Physica D **158**, 1 (2001).
[37] B. P. Bezruchko, T. V. Dikanev, and D. A. Smirnov, Phys. Rev. E **64**, 036210 (2001).
[38] H. U. Voss, in *Nonlinear Dynamics and Statistics*, edited by A. Mees (Birkhaeuser, Boston, 2001), pp. 413–434.